14 Intraoperative Urologic Ultrasound

Fernando J. Kim, Kyle Rove, and David E. Sehrt

Types of Transducers (Fig. 14.1)

Linear: The linear array scanners produce sound waves parallel to each other which generate a rectangular image. The width of the image and number of scan lines are the same at all tissue levels. Thus coupled with high-frequency settings, this probe has great near-field resolution. The linear transducer can be used for viewing surface texture of the liver. The disadvantage of this probe is the tendency for artifacts when applied to a curved part of the body which generate air gaps between skin and transducer.

Sector/vector: It produces a fanlike image that is narrow near the transducer and increases in width with deeper penetration. It is useful when scanning between the ribs as it fits in the intercostal space. The disadvantage is poor near-field resolution.

Curved: The curved probe is a compromise of the linear and sector scanners. The density of the scan lines decreases with greater distance from the transducer, but not to the level as sector scanners. Often imaging requires greater depth of the acoustic waves, so lower frequencies (3–5 MHz) are used. This lower frequency also allows scanning for patients with various body habitus. The curved probe may be difficult to use in curved regions of the body, e.g., the spleen behind the left costal margin.

Laparoscopic ultrasound (*LUS*): Laparoscopy with the assistance of ultrasound avoids unnecessary open surgery and improves selection of patients for renal and adrenal tumor resection. The diameter is less than 10 mm to allow introduction through a 10–11-mm laparoscopic port. The length is typically 35–50 cm and with articulating tips to allow imaging to any location in the abdominal cavity. LUS enables direct contact of the probe with the target tissue thus enabling the use of high-frequency (6–10 MHz) waves to improve resolution with a depth of 4–10 cm. LUS may be used to identify and characterize tumors, guide biopsy needles, probes, and monitor the freezing zone during cryoablation. Challenges of LUS include limitations of the small working space resulting in images from oblique planes.

Transrectal ultrasound: (a) *End fire* is a linear array whose direction of maximum radiation is along the axis of the array; it may be either unidirectional or bidirectional; the elements of the array are parallel and in the same plane, as in a fishbone antenna. (b) *Biplane is* composed of two arrays: one linear for imaging of the longitudinal plane and a highly curved one to image the

F.J. Kim, MD, FACS (✉) • D.E. Sehrt, BS
Department of Surgery/Urology, University of Colorado Health Science Center, Denver Health Medical Center, Tony Grampsas Cancer Center, 777 Bannock Street MC 0206, Denver, CO 80204, USA
e-mail: fernando.kim@dhha.org

K. Rove, MD
Department of Urology, University of Colorado Health Science Center, Aurora, CO, USA

P.F. Fulgham and B.R. Gilbert (eds.), *Practical Urological Ultrasound*, Current Clinical Urology,
DOI 10.1007/978-1-59745-351-6_14, © Springer Science+Business Media New York 2013

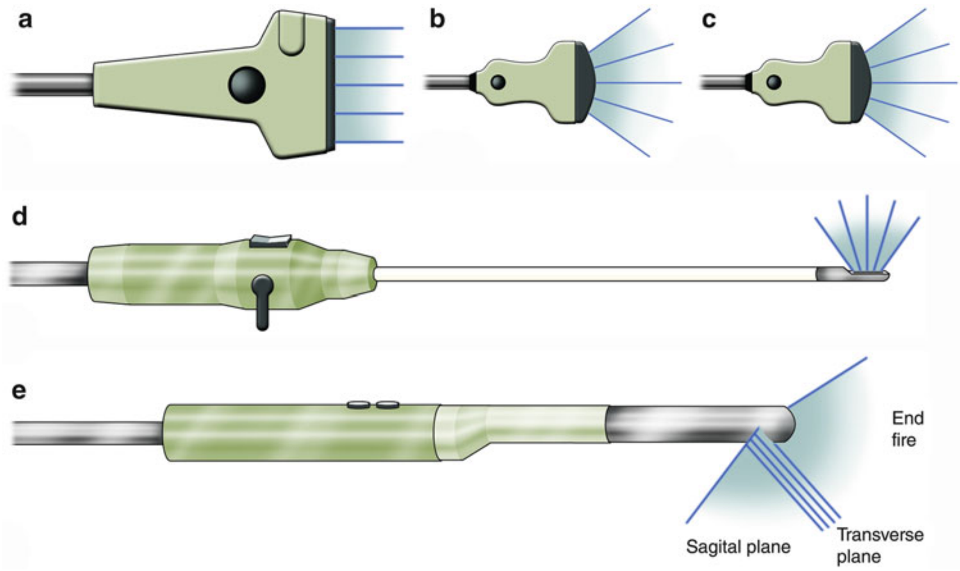

Fig. 14.1 Ultrasound probes used in urology. (**a**) Linear array (**b**) section/vector (**c**) curved array (**d**) laparoscopic (**e**) transrectal biplane

transverse plane. These two planes allow simultaneous visualization of perpendicular planes in real time.

The Kidneys

The same principles and techniques to perform renal procedures guided by ultrasonography apply to interventional techniques.

Percutaneous Nephrostomy and Percutaneous Nephrolithotomy

Percutaneous access to the renal collecting system was first described in 1955 by Goodwin et al. as a means to either drain or stent an obstructed urinary system [2]. Beyond the usual indications for an obstructed urinary system, percutaneous nephrostomy (PCN) can be used to access the collecting system in an antegrade manner for definitive treatment of nephrolithiasis, commonly performed by laser lithotripsy [3]. Generally, for percutaneous approach the left kidney is more challenging than the right due to the rib cage as described previously during the Kidney US chapter. Reports show that only 11% of urologists perform their own PCN access and majority uses fluoroscopic guidance, but given appropriate training and use of ultrasound guidance, this technique still remains well within the realm of the urologist as seen in some European and Asian countries [4–6].

Ultrasound probe: For adult abdominal scanning, a curved-array transducer 3–5 MHz is used. For pediatric patients, a higher-frequency transducer may be utilized. The use of color Doppler provides good visualization of vascular structures within the kidney, and the probes usually allow attachments that can display the path of the needle towards the target (calyx or stone).

Technique: Hydronephrosis on ultrasound will demonstrate enlarged renal calyces and pelvis that appear black (hypoechoic), indicating the presence of fluid. While acute hydronephrosis generally does not affect renal parenchyma, chronic obstruction of the urinary tract can result in thinning of the renal cortex (atrophy) and blunting of the renal papillae. Renal stones are identified as hyperechoic structure on US with shadowing, and color Doppler can identify vascular structures (Fig. 14.2). Presence of these

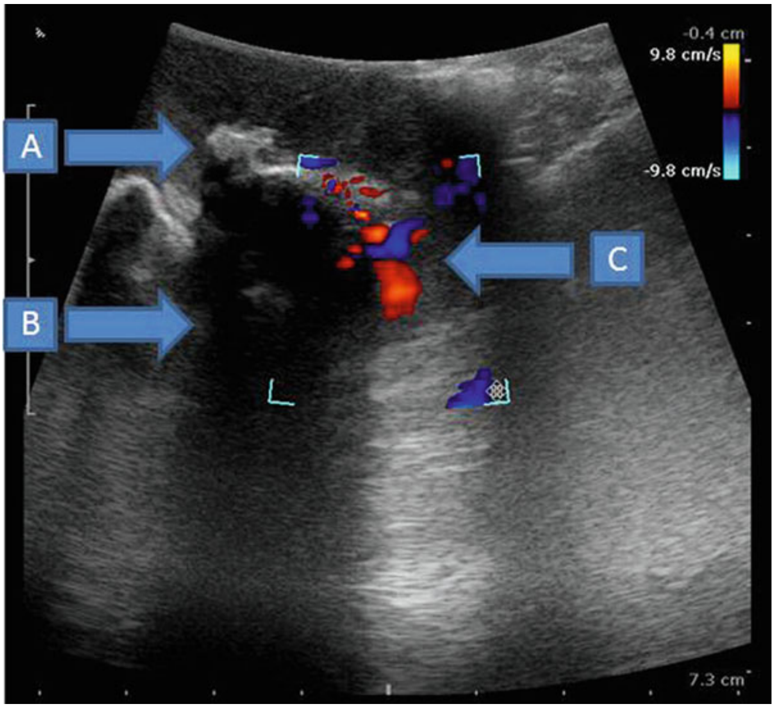

Fig. 14.2 Large hyperechoic renal stone with acoustic shadowing and color Doppler of vessels. (**a**) Large renal stone (**b**) acoustic shadowing (**c**) vessels on color Doppler

findings on ultrasound examination should be noted. Additionally, the operator should attempt to visualize the ureter, which may be dilated depending on etiology.

There are several described techniques, but the two most common are a one-stab technique and the Seldinger technique for placement of a PCN tube. The one-stab technique is usually reserved for moderately to severely dilated collecting systems. Meanwhile the Seldinger technique can be applied with or without dilation of the tract [7]. Both techniques are performed with the patient in a prone, prone-oblique position (Fig. 14.3). Recently, the supine position has been popularized for percutaneous nephrolithotomy (PCNL) [8]. The one-punch technique involves the use of ultrasound imaging to guide placement of a hollow 18-gauge needle with a sharp, beveled edge mounted to a pigtail catheter. Once inserted into the hydronephrotic collecting system and a flash of urine is obtained, the catheter can be slid over the needle and the needle subsequently removed [9]. Real-time ultrasound is used at all times to monitor the target and

Fig. 14.3 Percutaneous nephrolithotomy with needle-probe attachment. *Blue* marking of ribs

ensure that the needle, wire, and dilators enter the calyx and do not violate other structures (Fig. 14.4). If only drainage is needed, a 12-French PCN tube can then be inserted over the wire with curl confirmation on ultrasound imaging. Imaging can be enhanced by injecting sterile saline to identify the collecting system under US guidance. Further serial dilation or inflating balloon dilators can be performed with dilators up to the size of the instrument sheath (24 °F), ensuring

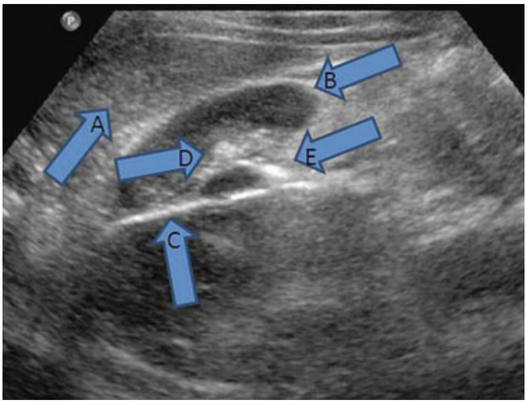

Fig. 14.4 Transverse view of the right kidney. (**a**) Liver (**b**) right kidney (**c**) percutaneous needle (**d**) collecting system (**e**) stone

that the wire remains in place for access purposes throughout the operation. In case of staghorn calculi, ultrasound guidance towards the stone or puncture of an alternate calyx may be required. The patient in a prone position allows the US probe to examine from the most lateral side of the abdomen under the rib cage and scan medially to enable a global view of the anatomy. The serious limitation of the ultrasound probe is the two-dimensional view of the kidney, calices, and the path which the needle may traverse injuring a viscera. The risk factors for colonic perforation are the following: the presence of colonic distension due to previous intestinal bypass surgery, female sex, elderly, thin patients, the presence of a horseshoe kidney, and previous renal surgery placing the colon in a more retroperitoneal position. The incidence of colonic injury is also greater on the left side, with a lower caliceal puncture, and with an extreme lateral origin of the percutaneous puncture [10]. Nevertheless, no statistically significant evidence has shown the implication of these factors in the development of colonic injury. Moreover, injuries to the spleen may occur on the left and liver on the right PCNL or PCN.

Clinical data: There has been one randomized trial that compared ultrasound-guided PCNL access to traditional fluoroscopic access and found comparable results with less exposure to ionizing radiation but longer access time (11.0 min vs. 5.5 min) [11]. In a large series of ultrasound-guided PCN by urologists, complications included urinary tract infection (1.1%), hemorrhage (1.9%), sepsis (0.76%), inferior vena cava injury (0.15%), gall bladder injury (0.15%), and death (0.3%). Overall, major complications occurred in 3.3% of patients (3–6.7% in various series) and minor complications in 5% (5–38% in various series) [12–14]. Successful PCN has been reported in these series as 90–95%. PCN and PCNL under ultrasound guidance are safe and highly successful techniques in the hands of a trained urologist.

Percutaneous Renal Biopsy

Renal biopsy can be divided in two groups of patients: (1) patients with an abnormal mass to rule out malignancy or (2) patients with medical renal disease that requires histologic diagnosis. In both groups of patients ultrasound imaging aids significantly to identify the suspected area. As discussed in other chapters of this book, the left renal US is often more challenging than the contralateral side due to the anatomic position.

Ultrasound probe: The use of curved-array 3.5–5-MHz probes with or without color Doppler provides good visualization and allows attachments that can display the path of the needle placement towards the target.

Technique: The technique is similar to PCNL. The target is different: (a) solid mass to rule out malignancy or (b) renal cortex to evaluate medical renal disease. As a general rule, percutaneous renal biopsy can be easily performed in nonobese patients and also transplanted kidneys since they are placed in the iliac fossa. The technique is similar to percutaneous renal procedures. If the colon is causing visual obstruction, rotate the patient and scan the kidney from posterior to anterior until the target is visualized. Preparation of the patient by fasting the night prior to the procedure may further improve visualization.

Clinical data: In the analysis of 623 renal biopsies guided by real-time ultrasound, the effectiveness was 97.6% with 110 complications. Fourteen (2.24%) were major complications (Clavien ≥3): 9 cases of renal hematoma, 2 cases with macroscopic hematuria (which required blood transfusion), 1 case of intestinal perforation (which required exploratory laparotomy), 1 nephrectomy, and 1 case of a dissecting hematoma. The author concluded that the risk factors for developing major complications were the following: diastolic blood pressure ≥90 mmHg, RR 7.6 (95% CI 1.35–43); platelet count ≤120 × 103/μL; RR 7.0 (95% CI 1.9–26.2); and blood urea nitrogen (BUN) ≥60 mg/dL, RR 9.27 (95% CI 2.8–30.7) [15].

Laparoscopic Ablative and Partial Nephrectomy

Historically, radical nephrectomy has been the treatment of choice for patients with renal masses, but our understanding and appreciation of nephron-sparing surgery for small renal masses ≤4 cm (and more recently, ≤7 cm in select patients) with regard to cancer control and preservation of renal function has increased dramatically in recent years [16–18]. There has been a recent migration towards nephron-sparing approaches as innovations with minimally invasive techniques continue [19]. The application of probe ablation therapies such as cryoablation and radio-frequency ablation, although promising, is currently not the treatment option of choice when compared to partial nephrectomy due the lack of long-term outcome data. Although percutaneous approach of the kidney for ablative procedures is feasible, the preferred imaging modality used to treat the renal masses by interventional radiologists has been CT scan. However amongst urologists, a laparoscopic approach using ultrasonography is more commonly implemented. Therefore, we will describe the use of laparoscopic ultrasonography for these procedures.

In the early 1990s, cryotherapy was reintroduced for the treatment of prostate cancer after study in animals and human trials in the 1970s and 1980s. On the basis of these experimental and clinical studies, an optimal drop in temperature of −40 °C is required to achieve total cell death [20]. Although many theories were suggested for the underlying mechanism of the cryoablative tissue effect, the vascular component of initial vasoconstriction followed by reperfusion injury (increased capillary permeability) triggered by the thawing phase is considered to be the primary mechanism of tissue damage. However, intracellular crystallization and subsequent water shifting during the thawing phase also contribute significantly to the rupture of the cell membrane and irreversible cellular death [21].

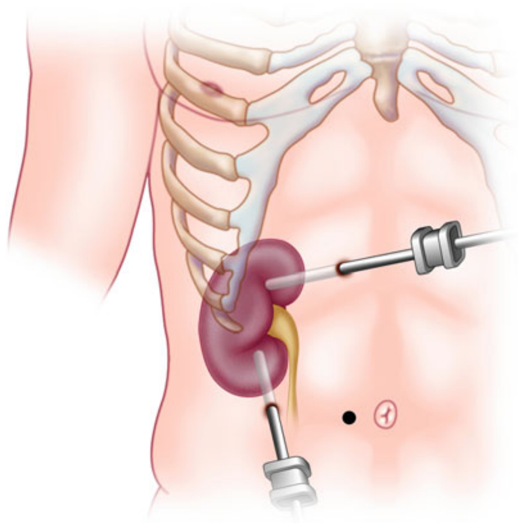

Fig. 14.5 Laparoscopic ultrasonic probe placement through a 10-mm trocar

Ultrasound probe: Laparoscopic renal ultrasound will often be performed with a 6–10-MHz linear array transducer. Endoluminal probes of 10–12 MHz may be used for transureteral evaluations. The 7.5-MHz flexible side-viewing laparoscopic transducer offers distinct capability to contour the organ. The rigid 7.5-MHz linear side-viewing laparoscopic transducer is easier to operate and is preferred by surgeons. Both types of transducers use a 10-mm laparoscopic port for introduction to the abdominal cavity (Fig. 14.5).

Technique: LUS imaging and orientation may not be intuitive and easy to understand the exact position of the lesion or particular regions of the target. The universal orientation left/cephalad also applies to LUS, but prior to the scan one should

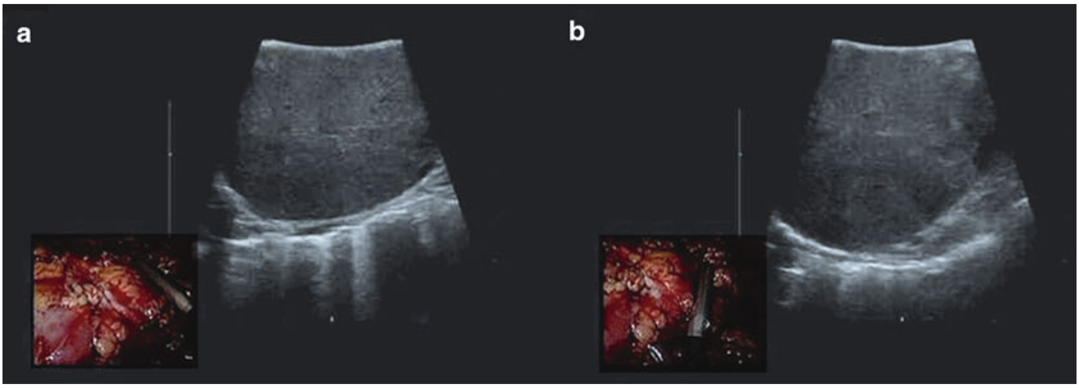

Fig. 14.6 Picture-in-picture of laparoscopic US during partial nephrectomy evaluates tumor size and depth to ascertain safe surgical margins. (**a**) lateral aspect of the renal tumor (**b**) medial aspect of the renal tumor

tip the end of the LUS to visualize the left side of the monitor and run along the crystals of the probe to translate the images of the US with the location in the monitor. For example, if only the tip of the LUS probe is touching the lesion, the image will be displayed only on the right side of the monitor. As the probe travels from the tip to the base of the probe, the image will be displayed in the entirety of the monitor (Fig. 14.6).

Indications for ultrasound-guided ablative therapy include small tumors (≤4 cm in diameter), older age, higher-risk patient, solitary kidney, and surgically scarred abdomen. Larger tumors and proximity to hilar vessels may be relative contraindications to ablative kidney surgery.

The size and optimal port placement are pivotal for LUS evaluation of renal lesions. The port size must be at least 10 mm. Generally, the posterior lesions are more challenging to be scanned. Either right or left side upper pole posterior lesions are best evaluated through an ipsilateral midclavicular or subxiphoid port. Anterior lesions can be evaluated almost through any port position. For a renal lesion biopsy and ablation, the needle or ablation probes are passed percutaneously through the abdominal wall. In general, multiple core biopsies (between 3 and 5) are taken with a 14- or 18-gauge needle under visual and ultrasonic guidance. Equally, the "rocking" maneuver allows the identification of the hyperechoic needle/probes and visualization of ablated tissue (Fig. 14.7).

Clinical data: A cryosystem consisting of argon (freezing phase) and helium (thawing phase) gases (Joule-Thomson effect) was used. Ultrasonic evaluation of the kidney should reveal suspect lesions. Simple cysts are generally spherical or ovoid, lack internal echoes, have a smooth, thin wall, and should show enhancement of the posterior wall indicating the presence of water. Lesions of suspect nature can include those with multiple septae, calcifications, or heterogeneous appearance that differentiates the lesion from healthy renal parenchyma [22]. The cryoneedles are introduced under real-time ultrasound guidance and will appear as hyperechoic structures with resultant shadowing. The borders of the ice ball can be readily identified on ultrasound as a hyperechoic rim (Fig. 14.8) which is generated by the interface between frozen and unfrozen tissues. The ice ball should be extended 1 cm beyond the visible border of treated lesions circumferentially to ensure negative margins. When thawed, the lesion will continue to remain hyperechoic compared with the surrounding kidney parenchyma [23]. All lesions should undergo two cycles of freezing and thawing.

The Adrenal Gland

Ultrasonography of the adrenal gland is technically difficult and is better evaluated by other imaging studies, i.e., CT scan and MRI [24]. LUS is a valuable adjunct to laparoscopic

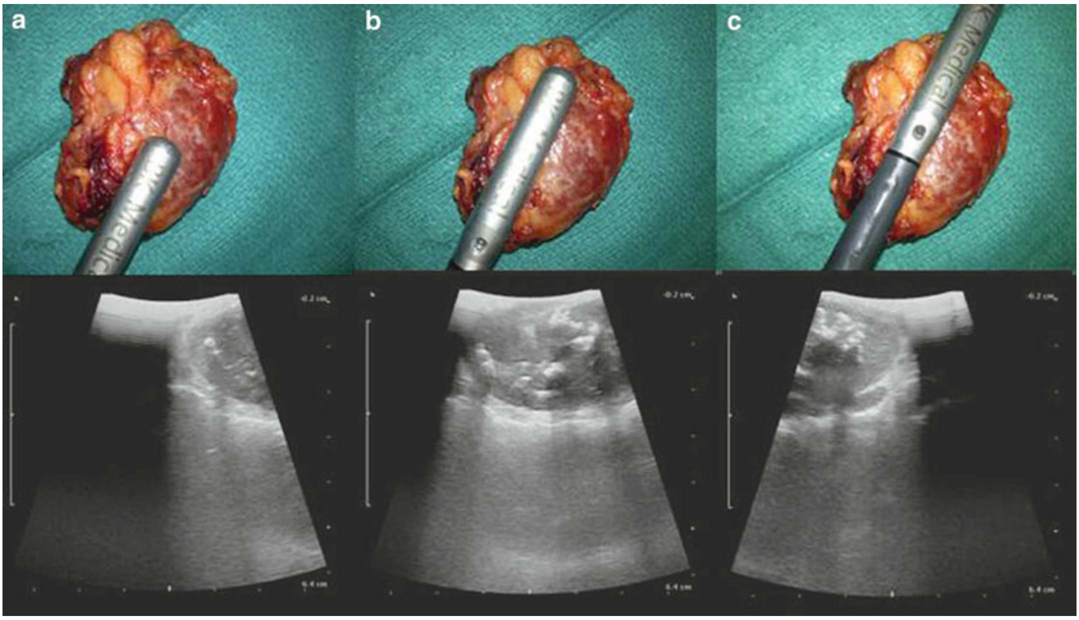

Fig. 14.7 Using the skiing technique across renal mass. The universal orientation of the laparoscopic probe is as follows: tip of the transducer is left and cephalad; therefore in (**a**) the distal end of the probe will demonstrate the adrenal mass on the right side of the monitor. When the transducer allows larger surface area contact, the image will show in the monitor (**b**) until only the base of the transducer is touching the adrenal mass and displaying the image on the left corner of the monitor (**c**) proximal end will demonstrate the adrenal mass on the left side of the monitor

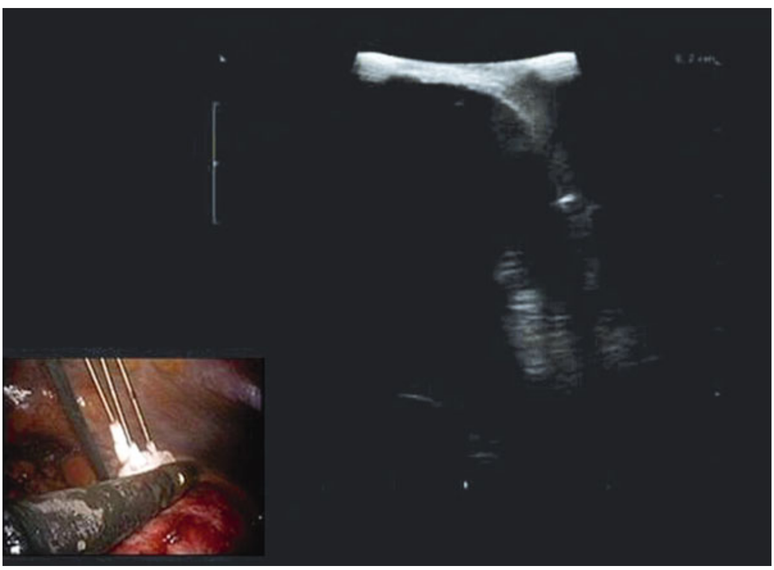

Fig. 14.8 Hyperechoic rim represents the outer layer of the ice ball. The homogeneous hypoechoic image is the ice ball that can be appreciated as the probes move towards the normal renal parenchyma

adrenalectomy facilitating tumor localization and identification of adjacent structures to direct the dissection particularly for partial adrenalectomies. Although large lesions on either side are easily identified, laparoscopic US may facilitate identification of small tumors in obese patients and right-sided lesions that are usually partially retrocaval.

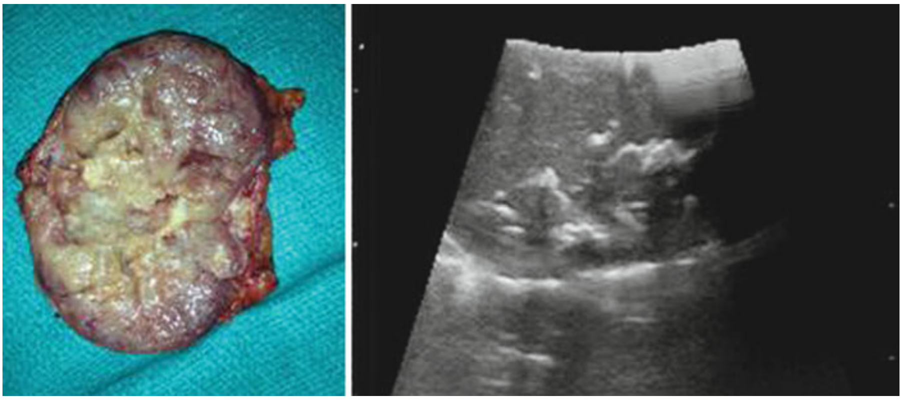

Fig. 14.9 An adrenal gland with ovarian metastasis. Gross anatomy with internal calcifications identified during laparoscopic adrenalectomy and use of LUS

Ultrasound probe: Although the flexible side-viewing 7.5-MHz rigid laparoscopic transducer offers distinct capability to contour the organ, often surgeons find the rigid, linear side-viewing transducer the simplest and most convenient to use in adrenal surgery.

Technique: In the transabdominal technique, the patient is placed in the modified flank position with 3–4 trocars inserted subcostally on the right and three trocars on the left, on an axis between the midclavicular and the midaxillary lines. After the dissection along the gutter to deviate the liver or the spleen medially to expose the suprarenal retroperitoneum, the laparoscopic transducer is inserted through the 10- or 12-mm port on the anterior axillary line or subxiphoid port. If the adrenal gland has not been identified, the upper pole of the kidney should be scanned demonstrating characteristic appearance of its parenchyma with the cortex and the collecting system. Then the transducer is advanced cephalad in the longitudinal plane until the adrenal gland is identified. Large tumors are easily identified and the value of intraoperative sonography in these cases is in elucidating their relationship with the kidney, aorta, spleen, and the tail of the pancreas on the left and the kidney, inferior vena cava, and the liver on the right side, respectively. The use of flow color Doppler also helps to identify the aorta and the inferior vena cava. Nonsecreting and secreting adenomas have a similar ultrasonographic appearance. They are usually less than 3 cm and have a very low echodensity. They sometimes contain cystic and calcified areas. Pheochromocytomas may appear as solid or cystic or may have both solid and cystic components. Hypoechoic areas represent necrosis and hyperechoic areas indicate hemorrhage. The ultrasound appearance of adrenal hyperplasia is of smooth enlargement with a normal echo pattern. Adrenal cortical carcinoma of 3–6 cm shows a homogeneous echo pattern similar to renal cortical tissue. Larger lesions vary in ultrasonographic appearance, having a heterogeneous appearance with focal or scattered hypoechoic or hyperechoic zones representing areas of tumor necrosis, hemorrhage, or, rarely, calcification. Metastatic adrenal tumors usually have an ovoid shape and variable echogenicity (Fig. 14.9). Adrenal cysts appear as anechoic masses with enhanced posterior sound transmission, whereas myelolipomas are highly echogenic because of their fat content. Although the use of LUS facilitates tumor evaluation and identification of adjacent structures, especially large vessels, in cases or pheochromocytoma and adrenal cortical carcinomas, compression of the adrenal gland may have very harmful effects either triggering catecholamine release or rupture of the malignant tumor causing spread of cancer.

Clinical experience: Contrast-enhanced ultrasonography has been employed in Europe and other countries to evaluate hypervascularity and correlate with malignancy. Hijioka et al. reported their experience on contrast-enhanced endoscopic ultrasonography (CE-EUS) to identify adrenal mass hypervascular lesions and perform EUS-guided fine needle aspiration (EUS-FNA). They concluded that this imaging modality can assist in the diagnosis of metastatic lesions, i.e., clear cell carcinoma leading to adrenalectomy and confirmation of metastatic clear cell carcinoma of the kidney [25]. Additional reports of ultrasound and/or CT scan-guided percutaneous cryoablation of adrenal masses have shown encouraging cost-effective outcomes. This procedure was associated with very low morbidity and local tumor recurrence rates and increased overall survival. Even as an adjunct to systemic therapies, it seems that percutaneous cryoablation of adrenal masses appeared cost-effective for palliation [26].

The Bladder

Suprapubic Tube Placement or Suprapubic Aspiration

Aspiration or trocar suprapubic tube placement (SPT) or "punch" suprapubic tube, as they are commonly referred, can offer quick drainage of the urinary bladder. The clinical scenario that necessitate SPT placement is the inability of the patient to void (posterior urethral disruption, urethral stricture) or when invasive urethral procedure may trigger sepsis (acute prostatitis) or autonomic dysreflexia (spinal cord injury patients) [27, 28]. The primary risk associated with this technique is perforation of bowel overlying the urinary bladder and open SPT approach must be applied in these patients.

Ultrasound probe: The use of curved-array 3.5–5-MHz probes with or without color Doppler provides good visualization and allows attachments that can display the path of the introducing needle towards the bladder. In the absence of this type of probe a linear array can be used to rule out bowel interposition between the skin and the bladder.

Technique: For ultrasound-guided trocar (SPT) placement or aspiration, the urologist should inquire the past surgical history of the patient, as prior abdominal operations could signify increased risk for bowel overlying the urinary bladder. On exam, the patient should have a distended bladder prior to the procedure and no scars that include the lower abdomen. Typical ultrasonography findings should include a variable-thickness bladder wall and dark homogeneous fluid content representing urine. One may survey the infraumbilical area and detect bowel contents represented by dark dynamic shadowing images representing peristalsis with gas content or any intervening tissue planes or heterogeneous echogenicity between the abdominal wall and urinary bladder. Presence of large blood clots also interferes with the hypoechoic characteristic of a full bladder. Further ruptured bladders will be difficult visualizing since the bladder may be empty. "Rocking" of the US probe will verify needle and catheter placement in a full bladder, and immediate urine drainage should be observed after initial puncture. The US probe follows the universal left/cephalad position and it should be positioned approximately three fingerbreadths above the pubic bone allowing the SPT needle to be placed between the US probe and the pubic bone (Fig. 14.10).

However some cases may require exploratory laparotomy, thus allowing for direct visual placement of suprapubic cystotomy tube. In instances where surgery is not needed, however, percutaneous SPT may be desirable. Trocar SPT or "punch" suprapubic tube, as they are commonly referred, can offer quick drainage of the urinary bladder. The primary risk associated with placement is perforation of bowel overlying the urinary bladder. While blind techniques have certainly been described in the past, modern access to ultrasonography can assist the urologist in an outpatient, operative, or emergency room setting in mitigating risk. Alternatives to straight ultrasound-guided placement include optional cystoscopic visualization and the previously mentioned open cystotomy and SPT.

For ultrasound-guided trocar SPT, the urologist or proceduralist should inquire as to the

Fig. 14.10 (**a**) Placement of a suprapubic catheter. (**b**) The clear visualization of the full bladder demonstrates no interposing bowel

patient's past surgical history, as prior abdominal operations could signify increased risk for adhesions, particularly with respect to bowel overlying the urinary bladder. On exam, the patient should have a distended bladder prior to beginning the procedure. Typical ultrasonography findings should include a variable-thickness abdominal wall and dark, fluid-filled urinary bladder.

Clinical data: A total of 140 pediatric patients less than 2 years old that required suprapubic aspiration (SPA) were randomized to either an ultrasound-guided or ultrasound-unguided (control) protocol. The aspirations under ultrasound guidance were performed under ultrasound examination during insertion of the needle. SPA had an overall success rate in 90% of attempts (63/70) in the ultrasound-guidance group compared with 64% (45/70) in the no-ultrasound group ($p < 0.05$). There were fewer passes made in those patients who had the procedure done under ultrasound guidance ($p < 0.05$). Ozkan et al. demonstrated the use of ultrasonography as an assistant tool for SPA in centers where portable ultrasound guidance is available, in particular, for infants more than 1 month old [29]. There are several clinical scenarios for SPT including traumatic injury (posterior urethral disruption, intraperitoneal bladder perforation), short-term use for neurogenic bladder, and urinary retention (as in setting of stricture or other bladder outlet obstruction) [27, 28].

The Prostate

Transrectal Ultrasound

The advent of US technology has improved visualization, and 3D reconstruction of the prostate via transrectal US is under development. The transrectal probes are slimmer and offer a real-time simultaneous sagittal and transverse view of the prostate. Moreover, the prostate can be visualized by either a suprapubic or transrectal approach. The former does not offer complete evaluation of the prostate but may assist to define the presence of an intravesical prostate. We have recently demonstrated the correlation of US anatomical findings and comparative cadaveric anatomy of the external urethral sphincter. The rhabdosphincter can be appreciated in the US images as a hyperechoic triangle at the apex of the prostate (Fig. 14.11), and the cadaveric models demonstrated a significant amount of muscle fibers overlapping the prostatic apex [30].

Ultrasound probe: A biplane or end-fire transrectal ultrasound probe with frequency range of 6.0–9.0 MHz should be used to evaluate the prostate and surrounding structures. Prostate size and morphology may also be evaluated using a trans-abdominal approach with a curved linear array probe. The transrectal probe should be able to accommodate a needle guide for transrectal ultrasound-guided biopsy. The needle guide may be a single-use or a reusable device.

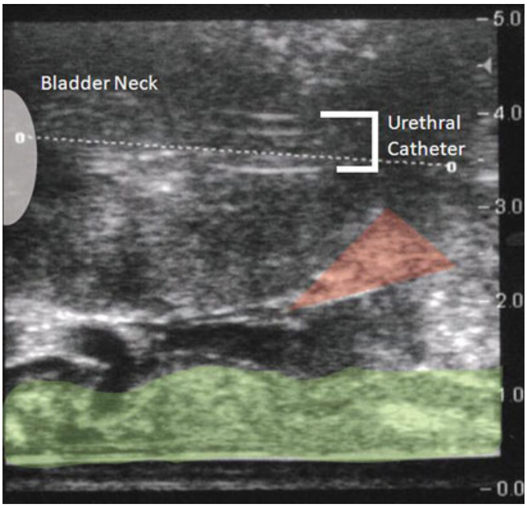

Fig. 14.11 Measurement of prostatic urethral length from the bladder neck to the prostate apex. The external sphincter is highlighted in *red*, the bladder neck in *white*, and the rectal wall in *green*

Technique: For optimal evaluation during transrectal ultrasound imaging, one must prepare the patient, giving instructions to clean the rectal vault. Presence of stool and gas compromises visualization. Fleet enema is recommended the night prior and the morning of the study. Slow introduction of the transrectal probe with lubrication in the rectum should be performed by gentle rotation and forward movement until the prostate is visualized. When a stepper is used, one may verify the correct model to use with different probes. Different techniques will be dependent on patient's position from lateral decubitus to lithotomy. The surgeon has to adjust and standardize images to transverse and sagittal views.

Transperineal Prostate Biopsies

The transperineal needle biopsy of the prostate is popular in Europe more than in the United States. While transperineal needle biopsy of the prostate was described as early as 1963, a grid-based, systematic, ultrasound-guided approach was not described until 2001 by Igal et al. Present biopsies involve the simultaneous use of image guidance via transrectal ultrasound with systematic sampling by either the standard sextant or whole gland mapping biopsies [31, 32]. Moreover, Barzell et al. describe extended biopsy technique with transrectal ultrasonography as an option for men with low-volume, low-grade, histologically proven prostate cancer who may be considering experimental targeted focal therapy. Prior to biopsy, the patient should undergo TRUS measurements of the prostate to ensure that the gland is not too large (<65 cm^3) and is not obstructed by the pubic arch. If the gland is too large or perineal access is partially obstructed, the patient can be started on 5α-reductase inhibitors and reevaluated every 3 months until the prostate is fully accessible. The procedure is generally performed in the clinic under local anesthesia with the patient in high lithotomy and use of a standard 5-mm interval brachytherapy perineal grid and a standard 18-gauge prostate needle biopsy gun. Five mm was determined to be the optimal grid size to ensure very few lesions are missed [33]. Cross-sectional ultrasound images are captured using a standard transrectal ultrasound probe, and these images are used to reconstruct the prostate in three dimensions by denoting borders of the gland. During the procedure, the urologist should note position of the urethra to avoid perforation with the biopsy gun. Care must be taken to ensure complete gland coverage by taking deeper (base) and shallow (apex) passes at the same grid position, as the length of the gland may be longer than a single pass of a standard 18-gauge biopsy needle. Each biopsy is labeled with x–y–z coordinates and placed in separate jars for histological analysis. Specialized software can then be used to combine pathology results (i.e., cancerous foci) with 3D model of the prostate generated from transrectal ultrasound images.

Cryotherapy

Cryotherapy was first proposed and used as a treatment for cancer in the nineteenth century. Using a combination of salt and ice applied to cervical and breast tumors, patients experienced less pain and decreased tumor size. Ultimately, conversion of air (oxygen and nitrogen) to their liquid forms and the ability to store them in adequate quantities for regular use brought about a resurgence in use in the early twentieth century. The first cryoprobe was built by Cooper and Lee in 1961 and circulated liquid nitrogen, allowing them to freeze tissues that were in contact with the probe, and the first use in the prostate was in 1964 [34]. The advent of ultrasound as a monitoring tool made cryotherapy as an ablative tool more attractive for the treatment of prostate cancer. The AUA recognized cryotherapy for localized prostate cancer as a standard treatment option in 1996. Current devices are labeled third generation and use urethral warmers, a combination of argon (cooling) and helium (warming) gases taking advantage of the Joule-Thomson effect, and TRUS guidance.

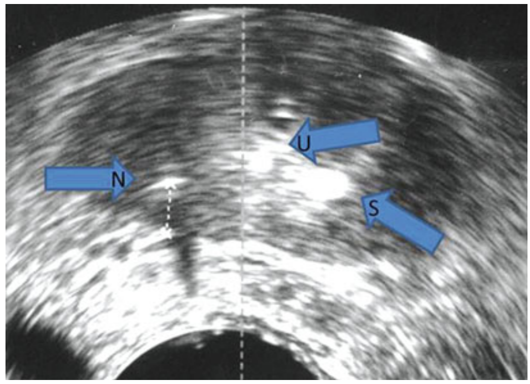

Fig. 14.12 Hyperechoic cryoablation needle (*N*) is observed and the distance to the prostate capsule may be measured. Additional left prostate stone (*S*) is visualized as well as the Foley catheter in the urethra (*U*)

Technique: With the patient in exaggerated lithotomy position, a brachytherapy template guide is placed on the perineum. A multifrequency biplanar transrectal ultrasound probe on a stepper is used for visualization of the prostate, urethra, bladder neck, and rectum. Temperature monitors are placed near Denonvilliers' fascia, external urinary sphincter, and neurovascular bundles, to monitor for appropriate level of freezing and avoid of thermal damage to these sensitive structures. Current recommendations state that temperature of these structures should remain above 15 °C. Cryoneedles are inserted under TRUS visualization into the grid to encompass either the entire gland or, in cases where focal therapy is desired, in the area of concern, identified by prior transperineal mapping biopsies (Fig. 14.12). Lastly, the urethral warmer is placed under cystoscopic guidance. For full-gland treatment, 2–4 mm of periprostatic tissues should be included in the treatment zone to ensure adequate cancer control. At the time of cystoscopy, the urethra is inspected for possible perforation of the needles or thermocouples, so that they can be moved prior to starting the freezing cycles. Freezing is carried out in an anterior-to-posterior direction to maintain TRUS visibility down to −40 °C for two freeze–thaw cycles. Visual guidance with ultrasound, though, has limitations that should be acknowledged prior to use [35, 36]. Ultrasound imaging cannot capture tissue temperature information during the procedure and changes visible in these images do not reliably correspond to specific temperature regions. Therefore, the temperature probes are placed before the cryoprobes. The identification of the external urinary sphincter must be well recognized by the surgeon to ensure proper probe placement to prevent urinary incontinence due to sphincter damage. We described the US findings and correlated with the studies in human cadaveric external urethral sphincter. The hyperechoic triangle distal to the apex of the prostate is the rhabdosphincter that has an important segment in the prostatic apex. The sphincter can be well demonstrated by pressing with the thumb over the base of the scrotum under the pubic arch [30]. Constant changes of views from sagittal to transverse and vice versa are required to evaluate the real-time progression of the ice ball to prevent rectal and urinary sphincter injury. The typical cryolesion is described as a well-marginated, hyperechoic rim with acoustic shadowing in the middle (Fig. 14.13). This hyperechoic rim obstructs the leading edge of frozen tissue, obscuring the true extent of affected area. Color Doppler may be useful to monitor blood flow around the rectum; however, this is not thought to be an objective monitoring tool. Complete thaw of the ice ball allows the visualization of the prostate as the beginning of the procedure.

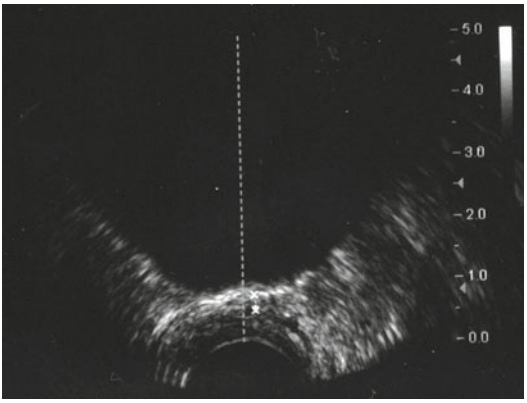

Fig. 14.13 Hyperechoic rim features of the external aspect of the ice ball during cryoablation of the prostate and the hypoechoic lesion representing the ice ball

Brachytherapy

Brachytherapy, or the placement of radioactive materials or seeds within the prostate, was first suggested by Alexander Graham Bell in 1908 [37–40]. Introduction of transrectal ultrasound-guided imaging offered the possibility of uniform distribution of the radioactive seeds for either permanent low-dose therapy (iodine-125, palladium-103) or temporary high-dose therapy (iridium-192) deposited into the prostate gland through a perineal template grid [41–43]. The introduction of image guidance also ensures seeds are not placed in close proximity to the urethra, nerves, or rectum, limiting side effects like lower urinary tract symptoms, erectile dysfunction, and fecal urgency. Ultrasound imaging during or at time of seed placement will generally reveal the hyperechoic needle and resultant shadowing. Similarly, seeds appear as small hyperechoic points. Assuring adequate dosimetry through appropriate placement of seeds remains paramount and has been shown to highly operator-dependent. However, computer-based planning systems coupled with TRUS imaging has allowed for precise and predictable seed placement that is reproducible (Fig. 14.14) [44]. Intraoperative preplanning replaces the need for an office visit with a planning session just prior to implantation in the operating room [45]. Because the exact number

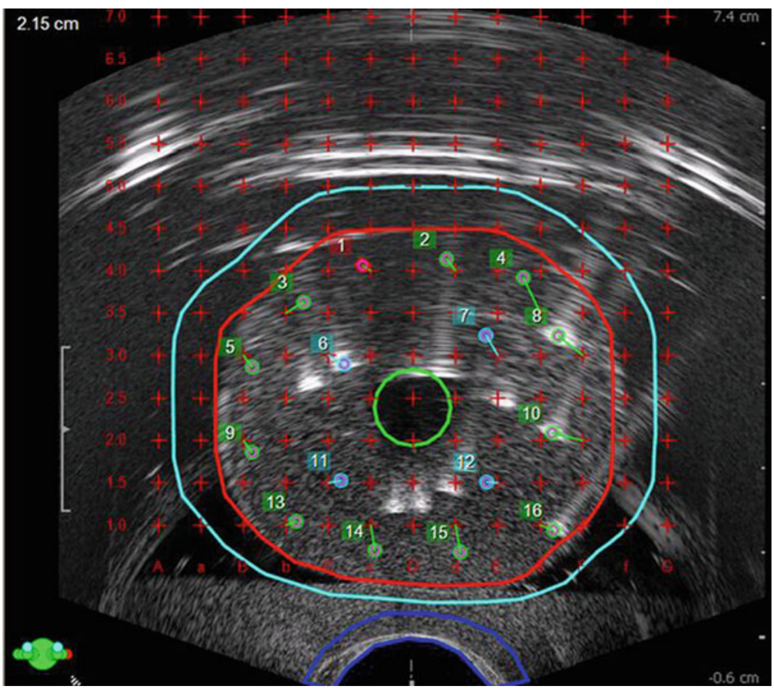

Fig. 14.14 Brachytherapy planning grid with positions of the brachy seeds. Seeds are visualized as hyperechoic objects

of required seeds is unknown prior to entering the OR, an approximate number are ordered according to a nomogram of gland volume derived from prior TRUS (at time of prostate biopsy) or CT. Biplanar TRUS imaging is performed in the exaggerated lithotomy position in the operating room and is fed to the treatment planning system. Transperineal implantation is then performed according to this plan. Biplanar TRUS imaging via US probe on a stepper is used to guide the needles throughout the procedure with confirmation of placement via fluoroscopy, since TRUS routinely cannot visualize anywhere from 2 to 45% of seeds during or after placement [46]. There are newer technologies that are under investigation looking at TRUS-fluoroscopy fusion imaging to verify seed placement and accurately verify dosimetry results during brachytherapy.

High-Intensity Focused Ultrasound

High-intensity focused ultrasound (HIFU) was first used over 15 years ago for the treatment of benign prostatic hypertrophy, and subsequently in 1996, Gelet et al. used this new technology for the treatment of patients with localized, low-grade adenocarcinoma of the prostate [47, 48]. HIFU is one such technique that can be used to focally ablate cancerous lesions using ultrasound energy to cause mechanical and thermal injury to the targeted tissue. HIFU, when used for the treatment of localized prostate cancer, uses a multifrequency ultrasound transducer placed in the rectum to generate acoustical energy that is focused on the tissue target, creating high temperatures and irreversible coagulative necrosis. HIFU utilizes a "trackless" principle, whereby tissue outside the focal plane is not damaged; the transrectal probe sits on the rectal mucosa and sends acoustical energy through the intervening tissues, only heating the tissue volume targeted by the probe [49]. The probe is repositioned mechanically as needed to target the prostate in its entirety. HIFU is performed with the patient placed under spinal or general anesthesia with prostate volumes greater than 40 cm^3 [50]. (Notably, study protocols of US trials do not permit the use of TURP prior to HIFU.) The prostate is visualized using real-time diagnostic images generated by the probe using lower, nondestructive acoustical energies (0.1–100 mW/cm^2). Once the target areas are identified, the prostate tissue is ablated with high energies (1,300–2,200 W/cm^2) focused in a small 1–3-mm-wide by 5–26-mm-long focal plane. Each pulse heats the tissue to 80–98 °C over a 3-s period. The gland is revisualized with lower ultrasound energies between ablative pulses. The probe is then moved and rotated in a semi-automated manner (device-dependent) using lower-energy diagnostic images to target adjacent prostate tissue. The end goal is to create overlapping lesions until the whole gland is treated. HIFU destroys target tissue through the thermal and mechanical effects of nonionizing, acoustical radiation (i.e., sound waves) delivered to target tissues after focusing by an acoustic lens, bowl-shaped transducer, or electronic phased array. Although not shown, the ablated area will become hyperechoic on lower-energy imaging. Because HIFU utilizes nonionizing radiation, it can be repeated one or more times during multiple sessions. The thermal effects are achieved by heating tissues to 60°C or higher, resulting in near-instantaneous coagulative necrosis and cell death [51]. By focusing the energy, more destruction occurs within the focal plane, but tissues outside the target area are spared of damage as energy intensities are far lower.

Laparoscopic Radical Prostatectomy

Ukimura, Gill, and colleagues recently described the use of real-time TRUS imaging of the prostate during laparoscopic prostatectomy, allowing for visualization of key structures such as the neurovascular bundles, bladder neck, and apex of the prostate, thus aiding in dissection [52].

Their report on intraoperative use of TRUS imaging for 25 consecutive patients notes the use of high-frequency 2D ultrasound imaging, power Doppler imaging, and 3D ultrasound imaging to aid in the identification of these key structures. In particular, the authors note that intraoperative use of ultrasound aided in three primary aspects of the laparoscopic prostatectomy. Ultrasound aided in identification of the correct plane between the posterior bladder neck and base of the prostate, thus allowing for laparoscopic visualization of seminal vesicles and vasa deferentia. Secondly, the authors described the ability to identify the distal protrusion of the prostate apex posterior to the membranous urethra in difficult cases, thus enhancing apical dissection to ensure negative margins. Finally, the authors note that intraoperative ultrasound offered the ability to identify hypoechoic nodules abutting the prostate capsule, allowing the surgeon to perform a wide dissection around these locations.

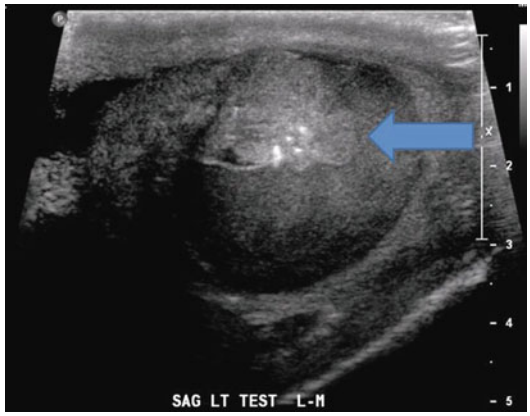

Fig. 14.15 *Blue arrow* depicts heterogeneous hyperechoic lesion of intratesticular mass (non-seminomatous germ cell tumor) with calcification

The Testis

Traditionally, patients with palpable or suspicious testicular masses would undergo radical orchiectomy, but investigators began to explore partial orchiectomy after intraoperative biopsy to confirm a lesion as benign or malignant, thus preserving testicular function in those where radical surgery is deemed unnecessary. Two recently published series show that the most common type of testicular tumor in prepubertal children is teratoma, a benign germ cell tumor (GCT).

Ultrasound probe: A high-frequency broadband linear transducer (4–12 MHz) can perform both power and spectral Doppler ultrasonography. Imaging of the scrotum, penis, and urethra is performed with a 7–12-MHz linear array transducer. The length of the transducer may vary from 4 to 8 cm. Equipment with Doppler capabilities is required for demonstrating blood flow in the evaluation of testicular torsion.

Technique: Technique and ultrasound probe for testis evaluation is described in detail in an earlier chapter. The linear array US is used intraoperatively after the testis is delivered via inguinal approach if malignancy is suspected. The cord is temporarily clamped and the testicle may be placed on ice (to minimize ischemia reperfusion injury) while the evaluation of the lesion is done. The goal is to delineate and determine respectability of the abnormal mass (hypoechoic/hyperechoic lesion compared to healthy parenchyma) (Fig. 14.15) that can be round or irregular and intratesticular. Dissection through the tunica albuginea and enucleation of the lesion with 2–5-mm margins should be carried out. The lesion should be sent for frozen section analysis by surgical pathology, and a determination of whether radical or partial orchiectomy is appropriately made. In the case of benign pathology, the tunica should be inspected for hemostasis and the incision closed. Finally, ultrasound may be used to inspect the affected area to ensure adequate resection of the lesion.

Clinical data: Organ-sparing approaches generally remain an option for a highly selected group of patients with testicular GCT only—men with bilateral testicular cancer or GCT in a solitary testis. Partial orchiectomy should be performed in such patients if the size and location of the mass are amenable to surgery. Partial orchiectomy of GCT provides a number of potential benefits over radical surgery: reduced need for androgen substitution, less psychological stress, preservation of fertility, and a durable cure rate. Partial orchiectomy of benign testicular lesions reduces the proportion of patients who are overtreated with radical orchiectomy. CIS detected in the testes remaining after partial orchiectomy can be treated with radiation therapy. Up to 40%

of patients will need hormonal replacement after this treatment. It should be emphasized that bilateral orchiectomy remains the best chance of cure in men with a solitary testis but comes at the cost of morbidity. Men should only undergo partial orchiectomy if one is certain that the lesion is benign. In this regard, size is important as masses larger than 2 cm in diameter are extremely suspicious for malignancy. Also, the lack of blood flow, serial growth, risk factors for GCT, and being impalpable all favor this approach [53].

The Renal Pelvis and Ureters

Stent Placement During Pregnancy and Patients in the ICU

Urolithiasis during pregnancy remains relatively common, affecting about 1 in 200 pregnancies [54]. While a majority of stones can be successfully managed conservatively with hydration, pain control, and antibiotics if necessary (70–80% will pass spontaneously owing mostly to physiologic dilatation of the ureters during pregnancy), the rest may require urologic intervention. Intravenous hydration may be necessary in cases of prolonged nausea and vomiting, and pain control should consist of acetaminophen with narcotic. Nonsteroidal anti-inflammatory medications should be avoided as they interfere with prostaglandin synthesis, which is required to maintain a patent ductus arteriosus until birth. In a portion of cases, renal colic and not urolithiasis may be the underlying cause of pain and necessitate urologic intervention [55]. Stent placement remains the most common of modern urologic interventions with various types of lithotripsy or PCN comprising the remainder. The urologist should note that stones and intervention may each increase the risk of preterm premature rupture of membranes and preterm labor. Minimally invasive techniques for managing patients who fail conservative treatment fall into two categories: temporary urinary drainage for obstructed urinary systems and procedures that facilitate stone removal. Stent placement has been performed using ultrasound guidance negating the need for ionizing radiation from intraoperative fluoroscopy and the concomitant risk to a fetus, particularly during the first trimester. When deciding on appropriate intervention for stones, diversion is usually recommended for stones that reside proximally in the collecting system [56]. Additionally, in cases of infected hydronephrosis or urosepsis, diversion is the mainstay of treatment. Cystoscopy for retrograde placement or PCN for antegrade placement of stents can be performed under local or regional anesthesia, thus minimizing the risk to the mother and fetus. Ureteral stents are placed at the time of cystoscopy, and ultrasound has been described as a valid tool for image guidance and confirmation of final stent position within the renal pelvis and bladder. Stent placement has been performed using ultrasound guidance negating the need for ionizing radiation from intraoperative fluoroscopy and the concomitant risk to a fetus, particularly during the first trimester.

Ultrasound probe: The use of a curved-array 3.5–5-MHz probe with or without color Doppler provides good visualization of the hydronephrosis calyx and or stone.

Technique: The technique, ultrasound probe, and limitations are similar to any renal ultrasound evaluation, with the special attention to the well-being of two instead of one patient. Fetal monitoring must be performed during the procedure with the assistance of the obstetric team. On renal ultrasound, stents appear as hyperechoic structures, and final placement with curls in the renal pelvis and bladder can be easily visualized as the cystoscope operator introduces and advances the ureteral stent up to the kidney. Additionally, one can evaluate the ureteral orifices with Doppler ultrasound of the bladder to confirm the presence of ureteral jets. Visualization of ureteral jets is an acceptable method of confirming the patency of the urinary tract. Patient can be awake or lightly sedated for the procedure with the assistance of the anesthesiologist and obstetric team to monitor the fetus. While one operator performs the cystoscopy, the radiologist or a second surgeon should perform the renal ultrasonography. The sonographer will

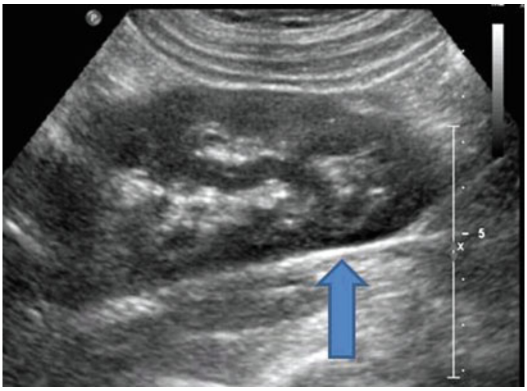

Fig. 14.16 Right ureteral stent placement under ultrasound guidance (*blue arrow*)

detect the hydronephrotic kidney and visualize the guide wire and stent placement real time (Fig. 14.16). Patients that are extremely unstable with septic shock due to impacted stone may have a stent placement using flexible cystoscopy and US guidance. In this case a single-J ureteral stent is preferable due to the stiffness and easier manipulation. Notably, stents should be changed every 4–6 weeks during pregnancy, as there is an increased propensity during pregnancy for stents to encrust.

Clinical data: One series of 300 pregnant women with renal colic, of whom 44 ultimately underwent ureteral stenting for symptomatic control or urinary obstruction, showed that stents placed during the second trimester were tolerated more (13/15 or 86.7%) as compared to those placed during the third trimester (14/26 or 53.8%) [55]. Our unpublished series includes five patients requiring ureteral stent placement in the intensive care unit. Three patients had a right-sided upper tract impacted stones, and two were left-sided (distal and mid ureter) stones. All patients were intubated and unstable. The use to flexible cystoscopy and single-J ureteral stents allowed prompt drainage of purulent urine and resolution of the septic shock. Placement of the left stents was more challenging due to the inability to move the patient to different positions and due to their high body mass index, but visualization of stent and flow during collection of intrarenal urine for culture was identified by color Doppler US. Moreover, the single-J stent allows repositioning that can be verified with simple abdominal X-ray (KUB).

Conclusion

Intraoperative use of ultrasound imaging has become standard in many different urologic interventions. Understanding its role in urologic surgery and interpreting key findings on ultrasound are essential to the successful use of this adjunct imaging technology. As newer devices, probes, and software are developed, we feel that use of ultrasound in the operating room will continue to expand into new areas.

References

1. http://www.auanet.org/content/guidelines-and-quality-care/policy-statements/c/consensus-statement-on-urologic-ultrasound-utilization.cfm.
2. Goodwin WE, Casey WC, Woolf W. Trocar (needle) nephrostomy in hydronephrosis. JAMA. 1955;157:891–4.
3. Gu Z, Qi J, Shen H, Liu J, Chen J. Percutaneous nephroscopic with holmium laser and ultrasound lithotripsy for complicated renal calculi. Lasers Med Sci. 2010;25:577–80.
4. Gupta S, Gulati M, Uday Shankar K, et al. Percutaneous nephrostomy with real-time sonographic guidance. Acta Radiol. 1997;38:454–7.
5. Bird VG, Fallon B, Winfield HN. Practice patterns in the treatment of large renal stones. J Endourol. 2003;17:355–61.
6. Skolarikos A, Alivizatos G, Papatsoris A, et al. Ultrasound-guided percutaneous nephrostomy performed by urologists: 10-year experience. Urology. 2006;68:495–9.
7. Alken P, Hutschenreiter G, Günther R. Percutaneous kidney stone removal. Eur Urol. 1982;8:304–11.
8. Miano R, Scoffone C, De Nunzio C, Germani S, Cracco C, Usai P, et al. Position: prone or supine is the issue of percutaneous nephrolithotomy. J Endourol. 2010;24:931–8.
9. Wah T. Percutaneous nephrostomy and antegrade ureteric stenting. Controversies and Consensus in Imaging and Intervention. 2005;3:20–2. Retrieved from www.c2i2.digithalamus.com (Feb 2012)
10. El-Nahas AR, Shokeir AA, El-Assmy AM, Shoma AM, Eraky I, El-Kenawy MR, et al. Colonic perfora-

tion during percutaneous nephrolithotomy: study of risk factors. Urology. 2006;67(5):937–41.
11. Basiri A, Ziaee A, Kianian H, et al. Ultrasonographic versus fluoroscopic access for percutaneous nephrolithotomy: a randomized clinical trial. J Endourol. 2008;22:281–4.
12. Radecka E, Magnusson A. Complications associated with percutaneous nephrostomies: a retrospective study. Acta Radiol. 2004;45:184–8.
13. von der Recke P, Nielsen MB, Pedersen JF. Complications of ultrasound guided nephrostomy: a 5-year experience. Acta Radiol. 1994;35:452–4.
14. Lewis S, Patel U. Major complications after percutaneous nephrostomy—lessons from a departmental audit. Clin Radiol. 2004;59:171–9.
15. Torres Muñoz A, Valdez-Ortiz R, González-Parra C, Espinoza-Dávila E, Morales-Buenrostro LE, Correa-Rotter R. Percutaneous renal biopsy of native kidneys: efficiency, safety and risk factors associated with major complications. Arch Med Sci. 2011;7:823–31.
16. Fergany AF, Hafez KS, Novick AC. Long-term results of nephron sparing surgery for localized renal cell carcinoma: 10-year followup. J Urol. 2000;163:442–5.
17. Lau WK, Blute ML, Weaver AL, Torres VE, Zincke H. Matched comparison of radical nephrectomy vs nephron-sparing surgery in patients with unilateral renal cell carcinoma and a normal contralateral kidney. Mayo Clin Proc. 2000;75:1236–42.
18. Huang WC, Levey AS, Serio AM, Snyder M, Vickers AJ, Raj GV, et al. Chronic kidney disease after nephrectomy in patients with renal cortical tumours: a retrospective cohort study. Lancet Oncol. 2006; 7:735–40.
19. Lee CT, Katz J, Shi W, Thaler HT, Reuter VE, Russo P. Surgical management of renal tumors 4cm or less in a contemporary cohort. J Urol. 2000;163:730–6.
20. Baust JG, Gage AA, Clarke D, et al. Cryosurgery—a putative approach to molecular-based optimization. Cryobiology. 2004;48:190–204.
21. Baust JG, Gage AA. The molecular basis of cryosurgery. BJU Int. 2005;95:1187–91.
22. Curry NS, Bissada NK. Radiologic evaluation of small and indeterminant renal masses. Urol Clin North Am. 1997;24:493–505.
23. Onik G, Reyes G, Cohen J, Porterfield B. Ultrasound characteristics of renal cryosurgery. Urology. 1993; 42:212–5.
24. Lockhart ME, Smith JK, Kenney PJ. Imaging of adrenal masses. Eur J Radiol. 2002;41(2):95–112.
25. Hijioka S, Sawaki A, Mizuno N, Hara K, Mekky MA, El-Amin H, et al. Contrast-enhanced endoscopic ultrasonography (CE-EUS) findings in adrenal metastasis from renal cell carcinoma. J Med Ultrason. 2011;38:89–92.
26. Bang HJ, Littrup PJ, Goodrich DJ, Currier BP, Aoun HD, Heilbrun LK, et al. Percutaneous cryoablation of metastatic renal cell carcinoma for local tumor control: feasibility, outcomes, and estimated cost-effectiveness for palliation. J Vasc Interv Radiol. 2012; 23:770–7.
27. Rosenstein D, McAninch JW. Urologic emergencies. Med Clin North Am. 2004;88:495–518.
28. Borrelli J, Brandes SB. Pelvic fractures: assessment and management for the urologist. AUA Update Series. 2004;23:82–6.
29. Ozkan B, Kaya O, Akda R, Unal O, Kaya D. Suprapubic bladder aspiration with or without ultrasound guidance. Clin Pediatr (Phila). 2000;39(10): 625–6.
30. Miano R, Kim FJ, De Nunzio C, Mauriello A, Sansalone S, Vespasiani G, et al. Morphological evaluation of the male external urethral sphincter complex by transrectal ultrasound: feasibility study and potential clinical applications. Urol Int. 2012; 89(3): 275–82.
31. Coppola R. Diagnosis of prostatic carcinoma by means of transperineal needle biopsy. Riforma Med. 1963;77:1282–4.
32. Igel TC, Knight MK, Young PR, et al. Systematic transperineal ultrasound guided template biopsy of the prostate in patients at high risk. J Urol. 2001; 165:1575–9.
33. Crawford ED, Wilson SS, Torkko KC, et al. Clinical staging of prostate cancer: a computer-simulated study of transperineal prostate biopsy. BJU Int. 2005; 96:999–1004.
34. Gonder MJ, Soanes WA, Smith V. Experimental prostate cryosurgery. Invest Urol. 1964;14:610–9.
35. Onik G, Cobb C, Cohen J, et al. US characteristics of frozen prostate. Radiology. 1988;168:629–31.
36. Littrup P, Monti J, Mody A, et al. Prostatic cryotherapy: ultrasonic and pathologic correlation in the canine model. Urology. 1994;44:175–84.
37. Scardino P, Carlton C. Combined interstitial and external irradiation for prostatic cancer. In: Javadpour N, editor. Principles and management of urologic cancer. Baltimore: Williams & Wilkins; 1983. p. 392–408.
38. Whitmore Jr WF, Hilaris B, Grabstald H. Retropubic implantation to iodine 125 in the treatment of prostatic cancer. J Urol. 1972;108:918–20.
39. DeLaney TF, Shipley WU, O'Leary MP, Biggs PJ, Prout Jr GR. Preoperative irradiation, lymphadenectomy, and 125iodine implantation for patients with localized carcinoma of the prostate. Int J Radiat Oncol Biol Phys. 1986;12:1779–85.
40. Aronowitz JN. Dawn of prostate brachytherapy: 1915–1930. Int J Radiat Oncol Biol Phys. 2002;54: 712–8.
41. Holm HH, Juul N, Pedersen JF, Hansen H, Stroyer I. Transperineal Iodine-125 seed implantation in prostatic cancer guided by transrectal ultrasonography. J Urol. 1983;130:283–6.
42. Ho A, Burri R, Cesaretti J, et al. Radiation dose predicts for biochemical control in intermediate-risk prostate cancer patients treated with low-dose-rate brachytherapy. Int J Radiat Oncol Biol Phys. 2009; 75:16–22.
43. Potters L, Roach III M, Davis B, et al. Postoperative nomogram predicting the 9-year probability of prostate cancer recurrence after permanent prostate brachyther-

apy using radiation dose as a prognostic variable. Int J Radiat Oncol Biol Phys. 2010; 76:1061–5.
44. Hinnen KA, Jan JB, van Roermund JG, et al. Long-term biochemical and survival outcome of 921 patients treated with I-125 permanent prostate brachytherapy. Int J Radiat Oncol Biol Phys. 2009;76:1433–8.
45. Nag S, Ciezki JP, Cormack R, et al. Intraoperative planning and evaluation of permanent prostate brachytherapy: report of the American Brachytherapy Society. Int J Radiat Oncol Biol Phys. 2001;51: 1422–30.
46. Han BH, Wallner K, Merrick G, Butler W, Sutlief S, Sylvester J. Prostate brachytherapy seed identification on post-implant TRUS images. Med Phys. 2003;30: 898–900.
47. Rove KO, Sullivan K, Crawford ED. High-intensity focused ultrasound: ready for primetime. Urol Clin North Am. 2010;37:27–35.
48. Gelet A, Chapelon JY, Bouvier R, et al. Local control of prostate cancer by transrectal HIFU therapy: preliminary results. J Urol. 1999;161:156–62.
49. Warwick R, Pond J. Trackless lesions in nervous tissues produced by high intensity focused ultrasound (high-frequency mechanical waves). J Anat. 1968; 102:387–405.
50. Chaussy C, Thuroff S. The status of high-intensity focused ultrasound in the treatment of localized prostate cancer and the impact of a combined resection. Curr Urol Rep. 2003;4:248–52.
51. Dewhirst MW, Viglianti BL, Lora-Michiels M, et al. Basic principles of thermal dosimetry and thermal thresholds for tissue damage from hyperthermia. Int J Hyperthermia. 2003;19:267–94.
52. Ukimura O, Gill IS, Desai MM, et al. Real-time transrectal ultrasonography during laparoscopic radical prostatectomy. J Urol. 2004;172:112–8.
53. Zuniga A, Lawrentschuk N, Jewett MA. Organ-sparing approaches for testicular masses. Nat Rev Urol. 2010;7:454–64.
54. Cormier CM, Canzoneri BJ, Lewis DF, et al. Urolithiasis in pregnancy: current diagnosis, treatment, and pregnancy complications. Obstet Gynecol Surv. 2006;61:733–41.
55. Andreoiu M, Macmahon R. Renal colic in pregnancy: lithiasis or physiological hydronephrosis? Urology. 2009;74:757–61.
56. Loughlin KR, Kerr LA. The current management of urolithiasis during pregnancy. Urol Clin North Am. 2002;29:701–4.